

INTERNAL ELECTROSTATIC DISCHARGE ENVIRONMENT AT JUPITER

Henry B. Garrett

The Jet Propulsion Laboratory, California Institute of Technology, 4800 Oak Grove Dr., Pasadena, CA 91109

O: 818-354-2644; F: 818-393-4699; Henry.Garrett@jpl.nasa.gov

Robin W. Evans

Gibbel Corp., 2550 Honolulu Blvd., Montrose, CA 91020

ABSTRACT

Although a fairly common occurrence in the Earth's environment, internal electrostatic discharge (or IESD) is seldom discussed with regards to extraterrestrial space missions. The Voyager 1 flyby of Jupiter, however, clearly demonstrated the importance of this phenomena in the context of the jovian radiation belts—Voyager suffered 42 Power-On Resets that were ultimately attributed to IESD during passage through the jovian belts. As several missions are being considered for the jovian environment, it is appropriate to revisit the effects observed on Voyager and review what we now know of the jovian IESD environment. In particular, NASA is considering a mission to orbit the moon Europa for the purpose of a close-up look at this possibly oceanic moon to determine if it might harbor life. This presentation will review the previous IESD observations from Voyager 1 in the context of our new understanding of the jovian radiation belts based on Galileo data.

INTRODUCTION

Although anomalies caused by internal electrostatic discharge (or IESD) are currently an important concern for Earth-based missions, IESD is not often considered as a hazard for interplanetary missions. During the Voyager 1 flyby of Jupiter, however, a number of anomalies were observed that were ultimately attributed to IESD. Indeed, IESD is a concern for any mission that must pass through a region of intense, high energy electrons such as found at the Earth and Jupiter. As several missions are currently being considered for the jovian environment, this paper will revisit the effects observed on Voyager and review what we now know of the jovian IESD environment based on Galileo observations. A specific example of a mission that could benefit from these findings is Europa Orbiter, a mission to orbit the jovian moon Europa. Following a brief discussion of the major issues associated with IESD, the jovian environment, and the original Voyager 1 observations, this paper will present several tools for evaluating IESD for both jovian orbiters and flyby missions. In addition, recent observations from Galileo in the vicinity of Europa will be discussed that shed light on the temporal variability of the jovian IESD environment. Together these results should provide a more complete understanding of the IESD threat around

one of the most important bodies in the solar system—Jupiter—and hopefully lead to more reliable spacecraft.

IESD

First consider the definition of IESD. Internal charging as used here refers to the accumulation of electrical charge on interior, ungrounded metals or on or in dielectrics inside a spacecraft. The key difference between “internal” and “external/surface” charging is that surface electrostatic discharges often are loosely coupled to victim circuits, whereas internal discharges may occur directly adjacent to victim circuits. Fig. 1 shows electron and proton ranges in aluminum versus energy. Since most satellites have an outer shell with aluminum equivalent thickness of 30 or more mils, internally deposited electrons usually have to have an external energy greater than 500 keV. Thus electrons with 500 keV of energy or more are considered to be the primary environment responsible for internal charging problems. Although the fluxes are normally lower at these higher energies, any internal electrostatic discharge (ESD) they might cause is closer to victim electronics than external ESDs and therefore can cause significant upset or damage to satellite electronics. Note, however, that “internal” charging can occur under thinner protective layers (as thin as a thermal blanket) so that the energy threshold for internal charging can be as low as 100 keV.

Except for bulk conducting materials, charge will be deposited over a finite depth—indeed, any particle with energy over a few eV will penetrate the surface. The depth of penetration and charge deposition is a function of stopping power, the energy of the impinging particles, and any electric fields normal to the surface. A common spacecraft surface configuration that will exhibit this behavior consists of an exposed dielectric material with a conductive backing connected to the spacecraft ground. Charge will accumulate (or diffuse away) in the dielectric over time as a function of the conductivity of the material and the imposed electric fields. If the charge accumulating in the dielectric induces a field greater than the breakdown strength of the material (typically of the order of 10^5 to 10^6 V/cm), a

discharge can occur within the material or from the interior of the dielectric to one of its surfaces.

Of equal importance in determining the likelihood of an IESD as the fluence is the time it takes for the electric field (E) to come to a constant value. That time period is characterized by the constant τ ($= \epsilon/\sigma$; σ is the conductivity in $(\text{ohm-m})^{-1}$ ($= \sigma_o + \sigma_r$); σ_o is the dark conductivity; σ_r is the radiation induced conductivity[1]; and ϵ is the dielectric constant). For many materials, τ ranges from 10 s to 10^3 s. Some common dielectric materials used in satellites have time constants of 3×10^5 s or more. In regions where the dose rate is high (enhancing the radiation conductivity), the E field comes to equilibrium rapidly. In lightly irradiated regions, where the time constant is long (the dark conductivity dominates), the field takes a long time to reach equilibrium. Depending on the dielectric constant and resistivity, as a rule of thumb, 10^{10} to 10^{11} electrons/cm² on the interior of a spacecraft may cause internal discharges (e.g., [2]). Electron energies of importance are between 100 keV to 3 MeV for typical spacecraft construction and most Earth orbits. Charging times at these energies and at the flux levels common to geosynchronous orbit would be about 3 to 10 hrs (jovian levels are discussed below). At lower charging rates, material conductivity often leaks off the charge so that internal charging would not be a problem.

DIVINE JOVIAN RADIATION MODEL

The next issue to be considered is the jovian radiation environment. Jupiter has the strongest magnetic field in the solar system. Since the ability to trap particles magnetically is a function of the magnetic strength, it is little wonder then that it has the most intense radiation belts yet observed. These belts are so intense in fact that they rival the man-made saturated nuclear environment at the Earth. To date, the principle engineering model of these radiation belts is the Divine formulation[3]. This model can be used to estimate the expected IESD electron fluence levels at Jupiter. (Note: as will be discussed below, the model is currently undergoing revision to reflect the recent Galileo observations of Jupiter though a revised model is at least a year away as data are still coming in.)

Jupiter has been known to have a magnetosphere since about 1960 when, in analogy with early spacecraft observations of the Earth's radiation belts, it was realized that the jovian UHF radio emissions could be interpreted in terms of trapped energetic electrons[4]. The successful encounters of the Pioneer 10 and 11 spacecraft with the jovian magnetosphere gave rise to a number of quantitative models describing various aspects of the jovian magnetosphere[5,6]. In particular, magnetic field

models by Smith et al.[7] and Acuna and Ness[8,9] began to delineate the substantial differences that exist between the jovian and terrestrial magnetospheres. Pronounced wave-like variations in the high energy particle fluxes led to the proposal that the jovian magnetosphere was distorted into a thin disc—the so-called magnetodisc theory—and that this thin disc was populated by a cold plasma consisting of heavy ions originating from Io. The passage of the Voyager 1 and 2 spacecraft further refined the particle and field observations. Subsequently, theoretical models have helped to interpret the observations and have led to the development of jovian magnetospheric models capable of being used to make practical predictions about the environment around Jupiter (see reviews [5,6]).

Based on remote radio emission data and in-situ particle data from the Pioneers and Voyagers, Divine[3] formulated a comprehensive engineering model of the jovian radiation environment suitable for IESD calculations. The basic variables in the model (e.g., magnetic L shell, local field strength B, pitch angle α with respect to the field line) are determined by Jupiter's magnetic field. A 15-coefficient, spherical harmonic magnetic field model, the O4 model derived from the fluxgate magnetometer on Pioneer 11[8,9], was used for this purpose to generate the radiation model components. For typical calculations, however, a simple dipole model is quite adequate. The dipole moment of that model was assumed to have the value $M=1.535 \times 10^{27}$ A m² = 4.218 G-R_J³. The value of the jovian equatorial radius was assumed to be 1 R_J = 7.14 x 10⁷ m. The common angular speed of rotation of Jupiter's internal magnetic field and of a meridian of constant longitude l in System III (1965) coordinates was assumed to be $\omega=870.536$ deg/day \approx 12.6 km/s R_J. In this system, l , the longitude, increases westward (opposite to the azimuthal angle in a system of spherical coordinates). Conversions to inertial and other coordinate systems may be derived from Seidelmann and Divine[10].

The principal radiation belt populations included in the model are, as in the case of the Earth, electrons (E>0.06 MeV) and protons (E>0.6 MeV). The range of applicability of the energetic electron model, the component of interest to this study, extends to the jovian magnetopause while that of the protons out to L=12. The electron model includes a pitch angle dependency within L=16 but is considered isotropic beyond that point. For the inner electron and proton models, the independent variables magnetic L shell, local field strength B, pitch angle α with respect to the field line, and particle kinetic energy E were utilized. The model populations are assumed independent of time,

longitude, and direction azimuth about the field line, as appropriate for stably trapped populations. The reader is referred to Divine and Garrett[3] for a complete description of the components of the model.

VOYAGER 1 POWER ON RESETS

During the Voyager 1 flyby of Jupiter on September 5, 1977[11,12], numerous anomalies were observed—most of which were determined to be related to 42 power-on resets (POR) within the Flight Data Subsystem (FDS). These were subsequently attributed to internal charging. In particular, it was postulated that ~MeV electrons had penetrated the surface of a cable and built up charge sufficient to cause arcing. Analysis of SCATHA, CRRES, and DSP data[13] showed similar effects. Laboratory studies by Leung[14], Frederickson[2,15,16], and others demonstrated that internal charging was a potential source of discharges. As a result, a series of IESD experiments were flown on the CRRES spacecraft in 1990-1991[2]. These experiments, which exposed a variety of configurations of isolated conducting surfaces and dielectrics to the Earth's radiation environment, demonstrated the reality of this effect. Typically, IESD occurred for fluences between 10^{10} - 10^{11} electrons/cm² in a 10 hour orbit.

Returning to the Voyager anomalies, the Voyager FDS was an on-board computer containing a volatile memory system. Pre-launch, there was concern that power-line undervoltage transients could cause malfunctions of the memory and computer operations with no warning of the malfunctions. To avoid the problem, a POR system was incorporated into the spacecraft's FDS. The key element was an undervoltage sensor that continually monitored the power supply voltage. If an undervoltage occurred, the sensor sent a digital signal to the delay logic electronics which stopped any processing, stopped the internal clock, reinitialized the computations as needed, waited a period of time, and then restarted computer activity if the undervoltage condition had ceased. The minimum period of time lost was about 175-ms. These 175-ms outages were identified by gaps in the data stream and by 175-ms discrepancies in the timing of spacecraft activities.

Fig. 2 illustrates the spatial distribution of the PORs. The timing of the PORs suggested an environmental origin as they occurred with greater frequency as the spacecraft went deeper into the Jupiter plasma environment and decreased as the spacecraft departed—the cause of the anomalies perhaps being electrostatic discharges. To validate this hypothesis, a ground test of the POR circuit was performed to determine its sensitivity to electrical transients. It was found that the sensitive element was an input buffer in

the processor delay logic circuitry located in an electronic circuit board about 20 cm away from the undervoltage sensor circuitry. As the interconnecting wiring was routed in common with other system wiring, it was postulated that ESD noise currents were carried by another wire into the spacecraft and passed near the POR interconnecting wiring. To test this, a 200-mA pulse with a risetime of 20-ns was injected into the adjacent 60-cm wire. This caused a 17-V, 20-ns pulse on the processor delay logic and triggered the circuit. An 8-A, 2- μ s current pulse caused a 3-V, 5- μ s voltage pulse on the processor delay logic warning and triggered the circuit. The current pulse slopes were 10- and 4-A/ μ s, respectively (that is, the rates were roughly comparable). Although not conclusive, these results support discharge as a likely cause of the POR upsets.

Estimates of surface charging in the jovian environment[11,17] indicated that surface charging was not the likely cause of the Voyager PORs. The predicted surface potentials did not follow the observed asymmetric anomaly pattern. In particular, the anomalies started at about 5.8 R_J on the inbound leg to perijove but continued occurring on the outbound leg to 9 R_J—well beyond the expected surface charging region. Rather it was proposed that the pattern might follow the time-integrated high energy electron fluence. To test this assumption, the total fluence of electrons at E>1 MeV and E>10 MeV and protons between 15<E<26 MeV were computed as a function of time. The resulting normalized curves are plotted versus the cumulative sum of Voyager POR anomalies in Fig. 3 (cumulative was used as the charge buildup associated with IESD is a cumulative process). Indeed, as this figure implies, IESD is a possible source of the Voyager anomalies in a temporal sense as the 10 MeV energetic electron fluence does roughly follow the pattern of POR events. The major evidence for buried charge as the cause, however, comes from an estimate of the charge deposited in each arc that would be necessary to cause the observed POR upsets. That argument is developed below.

As an estimate of the IESD environment encountered during the Voyager 1 flyby, consider the following:

- 1.) For 42 events in ~12 hrs-->
 $t \approx 10^3$ s/event
- 2.) For 4.5-9 R_J and 1 MeV electrons-->
 $J \approx 7 \times 10^7$ el/cm²-s
- 3.) \therefore Total available charge-->
 $Q(\text{event}) \approx 7 \times 10^{10}$ el/cm²-event

In the ground testing, a POR could be triggered indirectly by a current in a source wire adjacent to the

POR circuit wire by a current rising from 0 to 200 mA in 20 ns. The minimal charge to do this is calculated as:

$$1.) \Delta t \approx 20 \text{ ns}; I = 200 \text{ mA} \rightarrow$$

$$Q(\text{event})' \approx 5 \times 10^{-9} \text{ C} = 2 \times 10^{-9} \text{ C}$$

$$2.) \text{ As } 1 \text{ el} = 1.6 \times 10^{-19} \text{ C} \rightarrow$$

$$Q(\text{event})' \approx 1.3 \times 10^{10} \text{ el/event}$$

Although these values are probably only accurate to an order of magnitude, they imply that there should be sufficient electron fluence for $E > 1$ MeV onto a 1 cm^2 area behind a typical 2.03 mm (80 mil) aluminum surface to account for the observed Voyager 1 POR events. As discussed, Frederickson[2] found similar fluence levels in a 10 hour period were likely to generate IESD on the CRRES mission.

JOVIAN IESD TOOLS

In previous papers[3,18,19], simple “tools” were developed for helping projects determine regions of concern for surface charging at the Earth and Jupiter and IESD at the Earth. This paper adds tools for IESD at Jupiter. Figures 4, 5, and 6 are contour plots of the 1 MeV, 10 MeV, and 100 MeV electron fluences respectively at the indicated latitudes and radial distances in 10 hours. As such, these plots also provide rough estimates of the fluxes and fluences to be expected for circular orbits with those radii and inclinations. Given the 11° tilt and $0.1 R_J$ offset of the jovian magnetic field/radiation belts, the results for a specific circular orbit would be somewhat different and dependent on orbital phasing relative to Jupiter’s spin—levels would need to be calculated for the actual orbit. Even so, these three plots are useful for estimating when fluence levels might be high enough to cause IESD. For example, a spacecraft with a typical level of shielding of about 2.05 mm (80 mil) of aluminum (corresponding to ~ 1 MeV electrons) would likely begin to experience IESD anomalies for equatorial orbits inside approximately $10 R_J$ according to Fig. 4. At $\sim 2.2 \text{ cm}$ (corresponding to 10 MeV electrons) of shielding, the IESD problem appears to be minimal (the fluence would be less than 10^9 el/cm^2 in 10 hrs).

Voyager 1 is representative of another type of mission that could experience IESD—Jupiter gravity assist flybys. Figures 7 and 8 (based on data from Divine, 1991[20]) represent the peak fluxes and total fluences for jovian equatorial flybys with perijoves between $5 R_J$ and $50 R_J$ and electron energies from 0.1 MeV to 100 MeV. The peak flux can be used to estimate the worst IESD rate for a given perijove while the mission fluence can be used to estimate the total upsets. As an example, consider flybys for shielding levels of about 2.05 mm (80 mils) of aluminum. For

this shield thickness, the maximum flux within $10 R_J$ would be $\sim 10^8$ - $10^9 \text{ el/cm}^2\text{-s}$. At these levels, in a 1 hr period near perijove, a spacecraft might see 4-5 IESD events on an isolated interior conductor of $\sim \text{cm}^2$ area (similar to what Voyager 1 actually saw). Likewise, from Fig. 7, the total mission fluence for orbits with perijoves between 5 - $15 R_J$ is $\sim 10^{12}$ - 10^{13} el/cm^2 . This implies that a mission with perijoves in this range might see upwards of 10-100 events on the same isolated conductor as it passed by Jupiter. For a conductor behind $\sim 2.2 \text{ cm}$ (10 MeV or higher energy incident electrons) of shielding, there would likely be no upsets for a 1 cm^2 area. It would probably take upwards of 10 cm^2 area or more of a single conductor to cause an IESD.

GALILEO IESD

The apparent IESD effects on Voyager 1 were a major concern for the Galileo mission. As a result several steps were taken to limit these effects. To evaluate possible effects on Galileo, Leung[21] exposed representative samples of the spacecraft cabling and circuit boards to high energy electrons. The results demonstrated that IESD could be a real concern for isolated conductors on Galileo. To limit these effects, the approach taken by the project was to require all conductive surfaces to have a resistance of $< 10^{12} \text{ ohms}$ relative to spacecraft ground. Isolated conductors were limited to $< 3 \text{ cm}^2$. Ungrounded conductors with a length greater than 25 cm were also not allowed. It should also be noted that Galileo had an average shielding of 2.2 g/cm^2 (~ 300 mils or 0.75 cm of aluminum) corresponding to an electron cutoff of $\sim 3 \text{ MeV}$. As no obvious IESD events have been observed on Galileo, it appears that these steps were successful in eliminating IESD for the Galileo mission.

The Divine radiation model provides an “average” estimate of the IESD environment. Variations in the IESD environment might also be of concern, however. Fortunately, Galileo is currently providing real time measurements of the jovian environment. Specific to the IESD environment are high energy electron measurements by the Applied Physics Laboratory’s Energetic Particle Detector (EPD) at energies of 1.5-10.5 MeV, $E > 2 \text{ MeV}$, and $E > 11 \text{ MeV}$ [22]. In addition, recent work by Fieseler[23] has demonstrated that the Galileo Star Scanner is apparently sensitive to energetic electrons between 5-15 MeV electrons. While the EPD data will ultimately allow spectral measurements of the electron environment, there are numerous temporal gaps. The Star Scanner data on the other hand, while lacking in energy resolution, provide a near-continuous record over the Galileo mission. Using the two sets of data

averaged into 10 minute intervals, it has been possible to estimate the relative flux variations from orbit to orbit. Figure 8 presents these orbit to orbit variations for the mission up through January 2000 for the spatial interval 9-10 R_J near Europa's orbit. The key conclusion of this figure is that the high energy electron IESD environment appears to vary by a factor of ~2-3 around the average value from orbit to orbit. It is inferred from this that the IESD environment may also vary by a similar factor.

CONCLUSION

The objective of this study has been to provide an understanding of the expected IESD environment at Jupiter for future jovian missions. Jupiter is of interest to the space community as it has a severe radiation environment that is believed to have caused at least 42 IESD events during the Voyager 1 flyby. Based on the Divine model of the jovian radiation environment[3], a set of simple tools have been presented that allow estimates of the peak electron fluxes and mission fluences for both circular orbits and for equatorial flyby missions. The Divine model is an average model—to provide an estimate of the range of values, recent data from the Galileo mission in the vicinity of Europa were used to determine the expected temporal variations in the IESD environment. Based these results, a factor of 2-3 variation has been estimated. Finally, Galileo apparently has successfully avoided IESD anomalies by implementing a rigorous program that included limiting isolated conductors internal to the spacecraft radiation shield. The methods employed by Galileo to limit IESD were briefly discussed.

ACKNOWLEDGEMENTS

The authors would like to thank the Applied Physics Laboratory (W. McEntire and D. Williams) for providing the EPD data and P. Fieseler of the Galileo Project for providing the Star Scanner data. We also profited greatly from comments by our colleagues A. Whittlesey, R. Frederickson, and W. McAlpine of the Jet Propulsion Laboratory. The research described in this paper was carried out at the Jet Propulsion Laboratory, the California Institute of Technology, under contract with NASA.

REFERENCES

- [1]Frederickson, A.R., D.B. Cotts, J.A. Wall, and F.L. Bouquet, *Spacecraft Dielectric Material Properties and Spacecraft Charging*, AIAA Progress in Aeronautics and Astronautics, Vol. 107, American Institute of Aeronautics and Astronautics, Washington, D.C., 1986.
- [2]Frederickson, A.R., E.G. Holeman, and E.G. Mullen, "Characteristics of Spontaneous Electrical Discharges of Various Insulators in Space Radiation," *IEEE Trans. Nuc. Sci.*, Vol. V-39, No. 6, December, 1992.
- [3]Divine, T.N., and H.B. Garrett, "Charged particle distributions in Jupiter's magnetosphere," *J. Geophys. Res.*, Vol. 88, No. A9, Sept., pp. 6889-6903, 1983.
- [4]Drake, F.D., and H. Havatum, "Non-thermal microwave radiation from Jupiter," *Astron. J.*, Vol. 64, pp. 329-330, 1959.
- [5]Gehrels, T., ed. *Jupiter*. University of Arizona Press, Tucson, AZ, 1976.
- [6]Dessler, A.J., W.I. Axford, G.E. Hunt, and R. Greeley eds. *Physics of the Jovian Magnetosphere*. Cambridge Planetary Science Series, Cambridge University Press, New York, NY, 544 pages, 1983.
- [7]Smith, E.J., L. Davis Jr., and D.E. Jones, "Jupiter's magnetic field and magnetosphere," in *Jupiter*, T. Gehrels, Editor University of Arizona Press, Tucson, AZ, pp. 788-829, 1976.
- [8]Acuna, M.H., and N.F. Ness, "Results from the GSFC Fluxgate Magnetometer on Pioneer 11," in *Jupiter*, T. Gehrels, Editor University of Arizona Press, Tucson, AZ, pp. 830-847, 1976.
- [9]Acuna, M.H., and N.F. Ness, "The main magnetic field of Jupiter," *J. Geophys. Res.*, Vol. 81, pp. 2917-2922, 1976.
- [10]Seidelmann, P.K., and T.N. Divine, "Evaluation of Jupiter longitudes in System III (1965)," *Geophys. Res. Lett.*, Vol. 4, pp. 65-68, 1977.
- [11]Leung, P., A.C. Whittlesey, H.B. Garrett, P.A. Robinson Jr., and T.N. Divine, "Environment-Induced Electrostatic Discharges as the Cause of Voyager 1 Power-On Resets," *J. Spacecraft*, Vol. 23, No. 3, May/June, pp. 323-330, 1986.
- [12]Whittlesey, A.C., and P. Leung, "Space Plasma Charging--Lessons from Voyager," *AIAA 25th Aerospace Sciences Meeting, January 12-15*, Reno, NV, 1987.
- [13]Vampola, A.L., "Thick Dielectric Charging on High-Altitude Spacecraft," *J. Electrostatics*, Vol. 20, pp. 21-30, 1987.
- [14]Leung, P., "Discharge Characteristics of a Simulated Solar Array," *IEEE Trans. Nucl. Sci.*, Vol. NS-30, pp. 4311, 1983.
- [15]Frederickson, A.R., "Radiation Induced Dielectric Charging," in *Space Systems and Their Interactions*

with the Earth's Space Environment, H.B. Garrett and C.P. Pike, Editors, AIAA Press, New York, NY, pp. 386-412, 1980.

[16]Frederickson, A.R., "Electrostatic Charging and Discharging in Space Environments," *Proc. 10th Inter. Symp. Discharges and Electrical Insulation in Vacuum*, 1983.

[17]Garrett, H.B., and A. Hoffman, "Comparison of Spacecraft Charging Environments at the Earth, Jupiter, and Saturn," *IEEE Plasma Physics*, Vol. 28, No. 6, Special Issue on Space Plasmas, December, pp. 2048-2057, 2000.

[18]Evans, R., H.B. Garrett, S. Gabriel, and A.C. Whittlesey, "A Preliminary Spacecraft Charging Map for the Near Earth Environment," *Spacecraft Charging Technology Conference*, Naval Postgraduate School, 1989.

[19]Whittlesey, A.C., "Avoiding Problems Caused by Spacecraft On-Orbit Internal Charging Effects," NASA-HDBK-4002, NASA, 1999.

[20]Divine, N., "Flux, Fluence, and Dose for Jupiter Flyby Trajectories," IOM 5217-91-47, The Jet Propulsion Laboratory, February 25, 1991 .

[21]Leung, P.L., G.H. Plamp, and P.A. Robinson Jr., "Galileo Internal Electrostatic Discharge Program," *Spacecraft Environmental Interactions Technology 1983*, October 4-6, Colorado Springs, CO, NASA CP-2359/AFGL-TR-85-0018, 1983.

[22]Williams, D.J., R.W. McEntire, S. Jaskulek, and B. Wilken, "The Galileo Energetic Particle Detector," in *The Galileo Mission*, C.T. Russell, Editor Kluwer Academic Publishers, Dordrecht, The Netherlands, pp. 385-412, 1992.

[23]Fieseler, P.D., "The Galileo Star Scanner as an Instrument for Measuring Energetic Electrons in the Jovian Environment," Master's Thesis, University of Southern California, Los Angeles, CA, 2001.

FIGURES

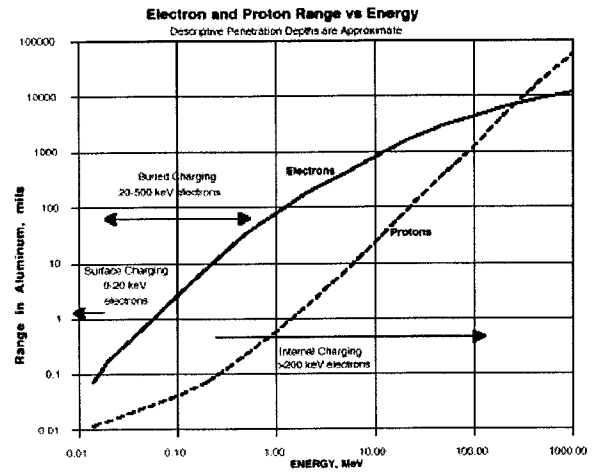


Fig 1. Approximate average electron and ion penetration ranges in aluminum[19].

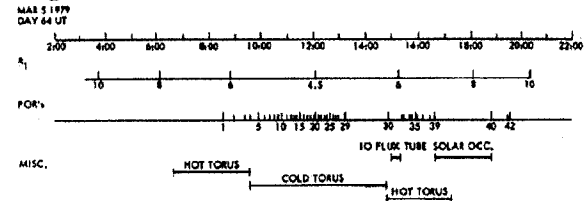


Fig. 2. Temporal and spatial occurrences of the 42 Voyager 1 POR anomalies during the March 5, 1979 flyby[11].

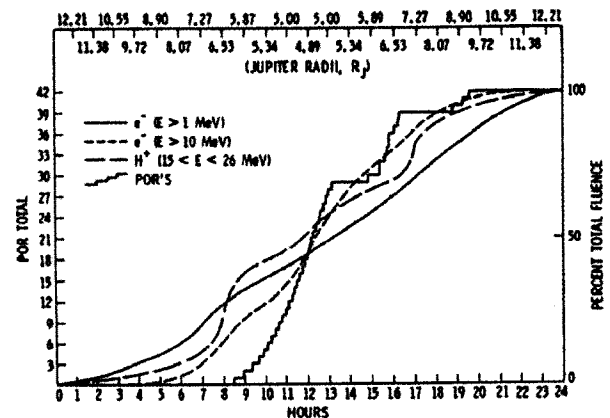


Fig. 3. Comparisons of the cumulative occurrence frequency of the 42 Voyager 1 POR anomalies versus the cumulative high energy electron ($E > 1$ MeV and $E > 10$ MeV) and proton ($15 \text{ MeV} < E < 26 \text{ MeV}$) fluences[11].

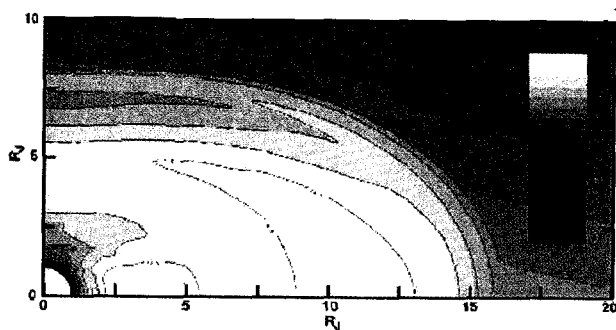


Fig. 4. Contour plot of the $E>1$ MeV high energy electron fluence environment at Jupiter as estimated from the Divine model. Fluences are for a 10 hr period.

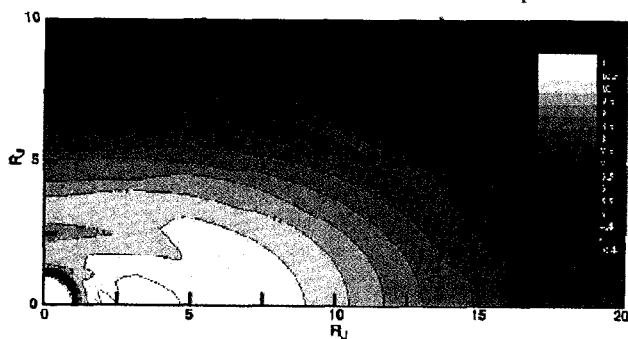


Fig. 5. Contour plot of the $E>10$ MeV high energy electron fluence environment at Jupiter as estimated from the Divine model. Fluences are for a 10 hr period.

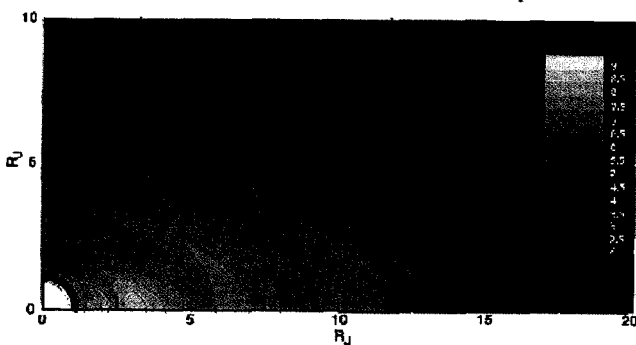


Fig. 6. Contour plot of the $E>100$ MeV high energy electron fluence environment at Jupiter as estimated from the Divine model. Fluences are for a 10 hr period.

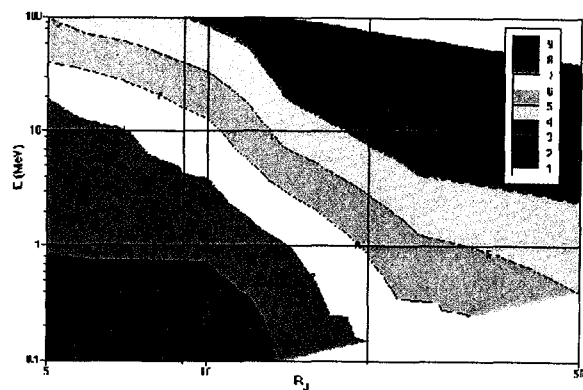


Fig. 7. Contour plot of the peak electron flux as a function of flyby perijove distance and energy (note: all flybys are assumed to be in the jovian equatorial plane)[20].

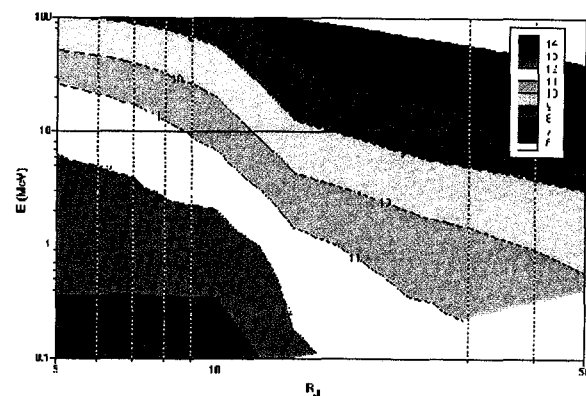


Fig. 8. Contour plot of the total electron fluence as a function of flyby perijove distance and energy (note: all flybys are assumed to be in the jovian equatorial plane)[20].

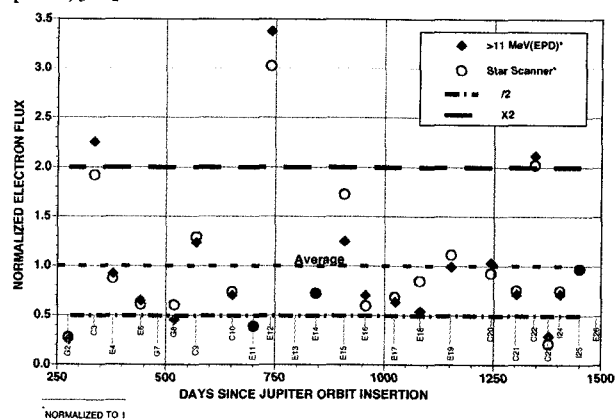


Fig. 9. Normalized energetic electron fluxes (10 minute averages) for $E>11$ MeV as measured by the Applied Physics Laboratory's EPD instrument on Galileo[22] up to January 2000. Also shown is the normalized Galileo Star Scanner background count rate (10 minute averages) for the same period[23].